

Assessing the connection between galactic conformity and assembly-type bias

Ivan Lacerna¹, Nelson Padilla^{2,3}, and Daniela Palma¹

¹ Instituto de Astronomía y Ciencias Planetarias, Universidad de Atacama, Copayapu 485, Copiapó, Chile
e-mail: ivan.lacerna@uda.cl

² CONICET. Instituto de Astronomía Teórica y Experimental (IATE). Laprida 854, Córdoba X5000BGR, Argentina

³ Universidad Nacional de Córdoba (UNC). Observatorio Astronómico de Córdoba (OAC). Laprida 854, Córdoba X5000BGR, Argentina

May 8, 2025

ABSTRACT

Context. Galaxies in the Universe show a conformity in the fraction of quenched galaxies out to large distances, being quite larger around quenched central galaxies than for star-forming ones. On the other hand, simulations have shown that the clustering of halos and the galaxies within them depends on secondary properties other than halo mass, a phenomenon termed assembly bias.

Aims. Our aim is to study whether samples that show galactic conformity also show assembly bias and to see if the amplitude of these two effects is correlated.

Methods. We use synthetic galaxies at $z = 0$ from the semi-analytical model *sag* run on the MultiDark Planck 2 (MDPL2) cosmological simulation and measure both conformity and galaxy assembly bias for different samples of central galaxies at fixed host halo mass. We focus on central galaxies hosted by low-mass halos of $10^{11.6} \leq M_h/h^{-1} M_\odot < 10^{11.8}$ because it is a mass range where the assembly bias has been reported to be strong. The samples of central galaxies are separated according to their specific star formation rate and stellar age.

Results. We find that the level of conformity shown by our different samples is correlated with the level of assembly bias measured for them. We also find that removing galaxies around massive halos diminishes the conformity signal and lowers the amount of assembly bias.

Conclusions. The high correlation in the amplitude of conformity and assembly bias for different samples with and without removing galaxies near massive halos clearly indicates the strong relationship between both phenomena.

1. Introduction

As part of the current effort to understand galaxy evolution, the environment in which galaxies reside is still a subject of intense study. The reason is that fundamental galaxy properties such as star formation rate and color can be affected by the environment, especially for low-mass galaxies (e.g., Peng et al. 2010; Bluck et al. 2014; Argudo-Fernández et al. 2018). Furthermore, low-mass galaxies show environmental effects on megaparsec scales, typically well beyond the virial radius of galaxy groups and clusters (e.g., Wetzel et al. 2012; Bahé et al. 2013; Benítez-Llambay et al. 2013; Cybulski et al. 2014; Campbell et al. 2015; Hearin et al. 2015; Bahé et al. 2017; Goddard et al. 2017; Zheng et al. 2017; Zinger et al. 2018; Duckworth et al. 2019; Kraljic et al. 2019; Pallero et al. 2019; Tremmel et al. 2019; Zheng et al. 2019; Pandey & Sarkar 2020; Zhang et al. 2021; Lacerna et al. 2022).

An example of the impact of the large-scale environment is the two-halo galactic conformity (e.g., Kauffmann et al. 2013; Hearin et al. 2015; 2016; Kauffmann 2015; Paranjape et al. 2015; Bray et al. 2016; Berti et al. 2017; Sin et al. 2017; 2019; Calderon et al. 2018; Lacerna et al. 2018; 2022; Rafieferantsoa & Davé 2018; Sun et al. 2018; Tinker et al. 2018; Treyer et al. 2018; Zu & Mandelbaum 2018; Alam et al. 2020; Li et al. 2021; Ayromlou et al. 2023; Olsen & Gawiser 2023; Wang et al. 2023; Palma et al. 2025). This term is used to describe the correlation between color or star formation activity in low-mass central galaxies, with stellar masses $M_\star < 10^{10.5} M_\odot$, and their neighbor galaxies in adjacent halos at separations of several megaparsecs. Kauffmann et al. (2013) found an observational two-halo confor-

mity effect between low-mass central¹ galaxies with low specific star formation rate (sSFR) or gas content and neighbor galaxies with low sSFR out to scales of 4 Mpc at $z < 0.03$. Cosmological hydrodynamical simulations (e.g., Bray et al. 2016; Wang et al. 2023), semi-analytic models of galaxy formation (e.g., Lacerna et al. 2018; 2022; Ayromlou et al. 2023), and semi-empirical models (e.g., Sin et al. 2017; Tinker et al. 2018) also show a correlation in color or star formation between central galaxies and neighboring galaxies at Mpc scales.

Using mock galaxy catalogs, Sin et al. (2017) found that the two-halo conformity out to projected distances of 3–4 Mpc from central galaxies primarily relates to the environmental influence of very large neighboring halos. Lacerna et al. (2022) demonstrated that the low-mass ($M_\star \leq 10^{10} h^{-1} M_\odot$) central galaxies that lie in the vicinity of massive systems are the ones most responsible for producing galactic conformity at Mpc scales. They used two galaxy catalogs from different versions of the semi-analytic model *sag* (Cora et al. 2018) applied to the MultiDark Planck 2 cosmological simulation (Klypin et al. 2016; Knebe et al. 2018) and the ILLUSTRIS TNG300 cosmological hydrodynamical simulation (Naiman et al. 2018; Nelson et al. 2018; Marinacci et al. 2018; Pillepich et al. 2018; Springel et al. 2018; Nelson et al. 2019), and consistently found that central galaxies in the vicinity of galaxy groups are primarily responsible for the correlation between the low-mass centrals and neighboring galaxies at large separations of several megaparsecs. Ayromlou

¹ They used galaxies without relatively bright neighbors as central galaxies.

et al. (2023) used a galaxy catalog from a semi-analytic model (LGal-A21, Ayromlou et al. 2021) and showed that the conformity signal, but not all of it, arises from central galaxies near massive systems.

On the other hand, Wang et al. (2023) found that low-mass central galaxies from the Sloan Digital Sky Survey (SDSS, York et al. 2000; Blanton et al. 2005) are more quenched in high-density regions, which generally contain a massive halo that would lie close to these low-mass galaxies. They also found a similar trend in ILLUSTRISTNG300, which, according to the authors, can be entirely explained by “backsplash”² galaxies. Recently, Palma et al. (2025) studied the evolution of low-mass central galaxies with $M_\star = 10^{9.5} - 10^{10} h^{-1} M_\odot$ near massive groups and clusters of galaxies using the ILLUSTRISTNG300 and MDPL2-SAG catalogs. They found that former satellites, that is, central galaxies at present that were satellites in the past, a simple way to define backplash or fly-by galaxies, play an important role in the two-halo conformity signal in ILLUSTRISTNG300. These galaxies can explain the whole signal at $z \sim 1$, while they contribute up to 75 – 85% at $z \lesssim 0.3$. They found a negligible contribution of former satellites to the conformity signal in MDPL2-SAG. Regardless of the specific contribution of former satellites, the results from these works are consistent in that the two-halo galactic conformity is primarily produced by low-mass central galaxies near massive halos with halo mass $M_h \geq 10^{13} M_\odot$.

Galaxy assembly bias is another phenomenon where the properties of a galaxy affect statistics on large separations well into the 2-halo scale regime. It is not unreasonable then to study both effects together, galaxy assembly bias and conformity. Galaxy assembly bias is often used to refer to the dependence of large-scale galaxy clustering on secondary halo properties beyond the halo mass. In the context of halo occupation distribution (HOD) modeling, galaxy assembly bias is described as the combination of assembly bias and the so-called occupancy variations, i.e., the dependencies of the galaxy content of halos on secondary halo properties at fixed halo mass (Artale et al. 2018; Zehavi et al. 2018; Contreras et al. 2019). Cosmological numerical simulations (semi-analytical models and hydrodynamical models) tend to show the existence of an assembly-type bias on synthetic galaxies (e.g., Croton et al. 2007; Lacerna & Padilla 2011; Wang et al. 2013a; Salcedo et al. 2018; Montero-Dorta et al. 2020). However, it is still unclear whether this effect is present in observations (e.g., Skibba et al. 2006; Cooper et al. 2010; Wang et al. 2013b; Lacerna et al. 2014; Lin et al. 2016; 2022; Dvornik et al. 2017; Oyarzún et al. 2022; 2024; Ortega-Martínez et al. 2024). See the review by Wechsler & Tinker (2018) on this topic.

Several works have suggested a relationship between the two-halo galactic conformity with the galaxy assembly bias as a potential manifestation of the large-scale environment on galaxies (e.g., Hearin et al. 2015; 2016; Berti et al. 2017; Paranjape et al. 2015; Lacerna et al. 2018; Mansfield & Kravtsov 2020; Montero-Dorta et al. 2020; Hadzhiyska et al. 2023; Damsted et al. 2024; Garcia-Quintero et al. 2025; McConachie et al. 2025). By using mock catalogs from the Bolshoi simulation, Hearin et al. (2015) scrambled the star formation rate (SFR) of satellite galaxies, which only marginally influenced the two-halo conformity signal on central galaxies out to $\sim 5 h^{-1} \text{ Mpc}$. They concluded that the conformity signal is driven by galaxy assembly bias on central galaxies. In contrast, Zu & Mandelbaum

(2018) used a “tunable” HOD to show that galactic conformity can be naturally explained by the combination of halo quenching and the variation of the halo mass function with the environment, without the need for any galaxy assembly bias. Paranjape et al. (2015) argued from extended HOD models for which only at separations larger than 8 Mpc there is genuine two-halo conformity driven by the assembly bias of small host halos.

One would be tempted to argue that since the conformity signal is typically limited to smaller scales, it would not correspond to assembly bias in principle. However, Hadzhiyska et al. (2023) conjectured that the galaxy formation process of Emission Line Galaxies (ELGs) may be dependent on the presence of nearby massive clusters, which in turn is connected with the two-halo conformity. They used ELGs extracted from the MillenniumTNG cosmological hydrodynamical simulation. It is possible that the level of assembly bias shown by ELGs in this simulation may be influenced by the conformity produced by nearby massive halos.

An explicit effort to assess the actual level of equivalence between galactic (or galaxy) conformity and assembly bias needs to be made since environmental effects in the vicinity of galaxy groups and clusters could be the cause of these two apparently different phenomena. For instance, Lacerna & Padilla (2011) claimed that assembly bias of low-mass systems can be explained by old, small structures located near massive halos that are typically at distances of a few megaparsecs. These massive halos could disrupt the growth of near-small objects with some mechanism (e.g., tidal stripping, Hahn et al. 2009) and, therefore, affect their properties, such as halo mass and formation time. There are similar concepts, such as “arrested development” (Dalal et al. 2008; Salcedo et al. 2018; Smith et al. 2024) or “neighbor bias”, in which the mean value of halo properties depends on, besides the halo mass, the distance to a massive neighbor and the ratio of that neighbor’s mass to the halo mass (Salcedo et al. 2018).

This work aims to make such an effort and explicitly look at the level of equivalence between conformity and assembly bias at large scales. For this, we use the MDPL2-SAG catalog to select central galaxies near massive halos that mostly produce the two-halo conformity in the low-mass regime, and study their direct contribution to the assembly-type bias signal. To avoid confusion with other definitions, we use the term assembly-type bias here, namely the secondary halo bias reflected in the clustering of central galaxies. The paper is organized as follows. Section 2 describes the synthetic galaxy catalog used in this work. The analysis of the two-halo galactic conformity is shown in Section 3, whereas the results on the assembly-type bias are shown in Section 4. We discuss our results and present our conclusions in Section 5.

Throughout this paper, the reduced Hubble constant, h , is defined as $H_0 = 100 h \text{ km s}^{-1} \text{ Mpc}^{-1}$. We opted for scaling h explicitly throughout this paper with the following dependencies unless the value of h is specified: stellar mass and halo mass in $h^{-1} M_\odot$, physical scale in $h^{-1} \text{ Mpc}$, and sSFR in $h \text{ yr}^{-1}$.

2. The MDPL2-SAG galaxy catalog

We use the MDPL2-SAG galaxy catalog constructed by combining the semi-analytic model of galaxy formation SAG (Cora et al. 2018) with the dark matter only MultiDark Planck 2 (MDPL2) cosmological simulation (Klypin et al. 2016; Knebe et al. 2018). The SAG code includes the contribution of several physical processes, such as radiative gas cooling, quiescent star formation, starbursts triggered by mergers and disc instabilities, ac-

² Wang et al. (2023) used the definition of main progenitors of central galaxies at present that were satellites of other halos for two successive snapshots.

tive galactic nuclei (AGN) and supernovae (SNe) Type Ia and II feedback, and chemical enrichment. The dark matter (DM) simulation assumes a Λ CDM cosmology with $\Omega_m = 0.307$, $\Omega_\Lambda = 0.693$, $\Omega_B = 0.048$, $n_s = 0.96$ and $H_0 = 100 h^{-1} \text{km s}^{-1} \text{Mpc}^{-1}$, where $h = 0.678$ (Planck Collaboration et al. 2014), tracing the evolution of 3840^3 particles from $z = 120$ to $z = 0$ in a box of side length $1 h^{-1} \text{Gpc}$.

The ROCKSTAR halo finder (Behroozi et al. 2013) was used to identify DM halos and their substructures. This algorithm is phase-space-based, searching for overdensities in the particle distribution in both position and velocity space, using a linking length of $b = 0.28$, guaranteeing that virial spherical overdensities can be determined for even the most ellipsoidal halos. In this context, any overdensities should comprise at least 20 DM particles. According to the selection criteria, central galaxies are identified as galaxies residing in the center of the potential well of host halos. These main structures can host multiple substructures called subhalos, where satellite galaxies reside.

The MDPL2-SAG datasets can be found in the COSMOSIM database³. From the public catalog, we use the positions, star formation rate (parameter ‘sfr’), the stellar mass as the sum of the mass of stars in the spheroid/bulge and the disk (parameters ‘mstarspheroid’ and ‘mstardisk’, respectively), and the stellar age with the parameter ‘meanagestars’, which is the mean age of the stellar population. For the host halo mass (M_h), we use the parameter ‘halomass’, which is the DM halo mass within a radius that contains a mean overdensity of 200 times the critical density of the Universe.

We focus on central galaxies at $z = 0$ hosted by low-mass halos of $10^{11.6} \leq M_h/h^{-1} M_\odot < 10^{11.8}$. The idea behind this selection is that all the analysis in the paper is at a fixed halo mass where assembly bias is strong (e.g., Gao et al. 2005; Li et al. 2008; Lacerna & Padilla 2011; Wechsler & Tinker 2018). The following section shows that these central galaxies show a remarkable signal of galactic conformity at large scales.

3. Two-halo galactic conformity

We measure the mean quenched fraction f_Q of neighboring (secondary) galaxies around central (primary) galaxies at fixed halo mass to assess the galactic conformity at $z = 0$. We use neighbor galaxies (either centrals or satellites) with stellar mass above $10^9 h^{-1} M_\odot$. This lower stellar mass limit has been used in other works with the MDPL2-SAG catalog to avoid resolution effects (e.g., Lacerna et al. 2022; Hough et al. 2023; Palma et al. 2025). We will refer to the fiducial primary sample with *all* the central galaxies at fixed halo mass as “PrimAll”. We remove central galaxies in the vicinity of massive systems of $M_h \geq 10^{13} h^{-1} M_\odot$ out to $5 h^{-1} \text{Mpc}$ to define a primary sample away from massive halos. These are the same samples used by Lacerna et al. (2022), who chose this particular scale as a simple representation of the large-scale environment beyond the virial radius of host halos (e.g., Argudo-Fernández et al. 2018; Kuutma et al. 2017). We will refer to this additional sample that does not include central galaxies around massive systems as “PrimB”.

We separated the galaxies into quenched (Q) and star-forming (SF) galaxies at $z = 0$. We consider the same sSFR cut used in Lacerna et al. (2022) and Palma et al. (2025) to split the samples. A galaxy is considered quenched if $\text{sSFR} \leq 10^{-10.5} h \text{ yr}^{-1}$. Otherwise, the galaxy is deemed to be star-forming.

This cut⁴ is chosen because it reproduces well the bimodality of galaxies in the MDPL2-SAG model, as shown in previous studies such as Brown et al. (2017) and Cora et al. (2018). We obtain a fraction of quenched galaxies of about 21 percent in the full catalog.

Figure 1 shows the mean quenched fraction of neighbor galaxies around central galaxies hosted by dark matter halos with masses between $10^{11.6}$ and $10^{11.8} h^{-1} M_\odot$. This figure is similar to that presented in Lacerna et al. (2022) and is also shown in this work for self-consistency. The solid lines correspond to all the central galaxies in the primary sample, case “PrimAll” (dark red and navy blue for quenched and star-forming primary galaxies). The dashed lines show the result after removing the central galaxies in the vicinity of halos more massive than $10^{13} h^{-1} M_\odot$ from the primary sample, case “PrimB” (red and blue for quenched and star-forming primary galaxies). The errors in the estimation of the mean fractions are calculated using 120 jackknives (e.g., Zehavi et al. 2002; Norberg et al. 2009). Error bars in the mean fractions are estimated by using the diagonal of the covariance matrix. Given the large number of galaxies, the error bars are small enough to be imperceptible in the figure.

The lower sub-panel of Fig. 1 shows the two-halo conformity signal for the two cases, measured as the difference of the mean quenched fractions of neighboring galaxies around quenched and star-forming primary galaxies (Δf_Q) at fixed halo mass. The signal is strong in the fiducial case where the fraction of quenched neighbor galaxies at distances of $\sim 1 h^{-1} \text{Mpc}$ from primary galaxies is much higher around quenched centrals than around star-forming centrals, with $\Delta f_Q = 0.22$. This correlation decreases with distance from the central galaxies, becoming quite low at distances $r \gtrsim 6 h^{-1} \text{Mpc}$ with $\Delta f_Q \lesssim 0.04$. In contrast, the two-halo conformity signal of the case “PrimB” is always very low at distances $r \gtrsim 1 h^{-1} \text{Mpc}$ with $\Delta f_Q \lesssim 0.02$. As shown by Lacerna et al. (2022), this result is not an artifact of removing galaxies from the primary sample. The low-mass central galaxies in the vicinity of galaxy groups and clusters are responsible for the majority of the conformity signal at megaparsec scales and show a larger neighbor quenched fraction than other centrals since, when removing these, the f_Q is also lower. In the next section, we will study their potential contribution to the assembly-type bias.

4. Assembly-type bias

In this section, we explore the contribution of low-mass central galaxies around massive groups and clusters to the assembly-type bias signal. As shown in the previous section, central galaxies hosted by low-mass halos near massive halos can greatly explain most of the two-halo conformity signal. Similarly to that approach, we first measure the two-point correlation functions for the fiducial case “PrimAll”, and then for the case “PrimB” that excludes the low-mass central galaxies in the vicinity of massive structures.

We use the software CORRFUNC (Sinha & Garrison 2017; Sinha & Garrison 2019; Sinha & Garrison 2020) to measure the two-point correlation functions using the Landy-Szalay estimator (Landy & Szalay 1993). Given the geometrical effect of removing galaxies out to clustercentric distances of $5 h^{-1} \text{Mpc}$, we have constructed a random catalog for the case “PrimB” that considers this effect. First, we created a fiducial random catalog

⁴ Notice that it corresponds to $\text{sSFR} \sim 10^{-10.7} \text{ yr}^{-1}$ with $h = 0.678$, close to other cuts commonly used in the literature, e.g., 10^{-11} yr^{-1} (Wetzel et al. 2012).

³ <https://www.cosmosim.org/>

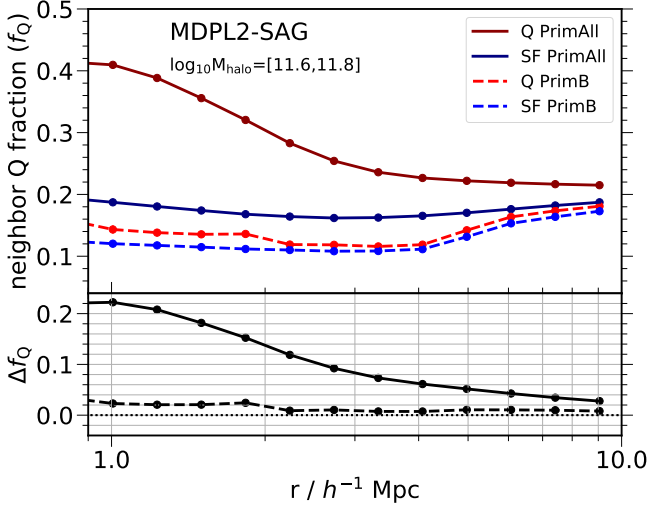


Fig. 1. The main panel shows the mean quenched fractions of neighboring galaxies as functions of the real-space distance from primary galaxies hosted by low-mass halos of $10^{11.6} \leq M_h/h^{-1} \text{ M}_\odot < 10^{11.8}$. The solid lines correspond to all the central galaxies in the primary sample, “PrimAll” (dark red and navy blue for quenched and star-forming primary galaxies). The dashed lines correspond to the mean fractions after removing the central galaxies in the vicinity of halos more massive than $10^{13} h^{-1} \text{ M}_\odot$ from the primary sample, case “PrimB” (red and blue for quenched and star-forming primary galaxies). The lower sub-panel shows the difference of the mean quenched fractions of neighboring galaxies around quenched and star-forming primary galaxies at fixed halo mass. The x-axis is the distance from the primary galaxies. The solid line shows the case “PrimAll”, whereas the dashed line is the result obtained for “PrimB”. The dotted line denotes the case of zero difference, i.e., no conformity.

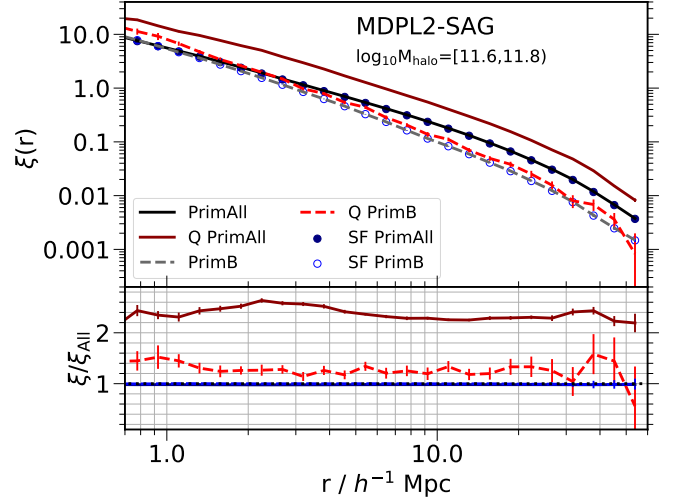


Fig. 2. The main panel shows the two-point correlation functions of primary galaxies hosted by dark matter halos with masses of $10^{11.6} \leq M_h/h^{-1} \text{ M}_\odot < 10^{11.8}$. The autocorrelation function for the case with all the central galaxies in the primary sample, “PrimAll”, is shown as a solid black line, whereas the dark red solid line and navy blue circles correspond to the cross-correlation functions of quenched and star-forming primary galaxies, respectively. On the other hand, the dashed gray line corresponds to the autocorrelation function after removing the central galaxies in the vicinity of halos more massive than $10^{13} h^{-1} \text{ M}_\odot$ from the primary sample, case “PrimB”. The red dashed line and open blue circles correspond to the cross-correlation functions of quenched and star-forming primary galaxies in the case “PrimB”, respectively. The dashed lines and open circles are then the results after removing the galaxies that mostly contribute to the two-halo galactic conformity. The sub-panel shows the ratio between the correlation function of quenched centrals (red) and the total population and between the star-forming centrals (blue) and the total population. The solid and dashed lines are for the cases “PrimAll” and “PrimB”, respectively.

within the simulation box that is three times the number of primary galaxies, producing a catalog of $\sim 8,200,000$ random objects. Then, we use the positions of groups and clusters in the simulation to remove the random points at clustercentric distances $\leq 5 h^{-1} \text{ Mpc}$ in real space. The random catalog of the case “PrimB” is made of the remaining random points (about $\sim 7,000,000$ objects). The error bars in the clustering estimations of this section are calculated using the diagonal of the covariance matrix from the bootstrap method (e.g., Norberg et al. 2009) by randomly resampling each galaxy sample 25 times with replacement.

4.1. Quenched and star-forming samples for a defined cut in sSFR

The aim of this sub-section is to assess the contribution of the galaxies that produce the two-halo conformity to the assembly-type bias signal using the same conditions of Section 3, i.e., we estimate the two-point correlation functions for the samples of quenched and star-forming primary galaxies defined in the previous section using a cut in sSFR of $10^{-10.5} h \text{ yr}^{-1}$. Given the low-mass regime of M_h between $10^{11.6}$ and $10^{11.8} h^{-1} \text{ M}_\odot$, the fraction of SF central galaxies is much higher than the fraction of Q central galaxies with the same host halo mass (98.5% and 1.5%, respectively). Sect. 4.2 will show the results for samples with the same number of quenched and star-forming central galaxies.

4.1.1. Fiducial case “PrimAll”

Figure 2 shows the two-point cross-correlation functions between the quenched primary galaxies and the full sample of primary galaxies (dark red solid line) and between star-forming primary galaxies and the full sample of primary galaxies (navy blue circles) in the case “PrimAll”. They correspond to the fiducial case of central galaxies hosted by low-mass dark matter halos between $M_h = 10^{11.6}$ and $10^{11.8} h^{-1} \text{ M}_\odot$. The overall clustering of central galaxies is expected to be dominated by star-forming galaxies because they correspond to the majority of the centrals in the halo mass range explored in this paper. This behavior is demonstrated when we show the autocorrelation function of all the primary galaxies in the fiducial case as a black solid line, with a clustering almost the same as the cross-correlation of the SF primaries (navy blue circles). On the other hand, the clustering of quenched central galaxies is higher than that of star-forming centrals hosted by halos of the same mass. This result is also seen in the solid lines of the bottom panel, which shows the ratio between the correlation function of quenched centrals and the total population (dark red) and between the star-forming centrals and the total population (navy blue) of the fiducial case. The ratio is a factor above 2 for the quenched central galaxies out to $50 h^{-1} \text{ Mpc}$, which implies a strong secondary bias on this population because the galaxy clustering depends on the sSFR at fixed halo mass.

4.1.2. Case “PrimB”

In Sect. 3, we mentioned the significant contribution of central galaxies in the vicinity of massive halos in the two-halo galactic conformity signal. To assess the contribution of these galaxies in the fiducial signal of the assembly-type bias shown in Sec. 4.1.1, we repeat the process of removing those galaxies from the primary sample, i.e., we estimate the two-point correlation functions for the case “PrimB”. The cross-correlation function between the quenched (star-forming) primary galaxies and the primary galaxies for this case is shown in the red dashed line (blue open circles) in the main panel of Fig. 2. The autocorrelation function of the primary galaxies of the case “PrimB” is shown as a gray dashed line. Star-forming galaxies still dominate the overall clustering of central galaxies because they correspond to 99.5% of the centrals in this case.

A difference compared with the fiducial case is that the clustering decreases for the quenched and star-forming populations, even when the halo mass range is the same, probably due to the removal of galaxies in the vicinities of massive halos. Furthermore, the difference in the clustering between the quenched and star-forming galaxies of the same halo mass is remarkably reduced, which is also shown by the correlation function ratios in the bottom panel of the figure in dashed lines. The average ratio in the two-halo regime between 1 and 50 h^{-1} Mpc is 1.28 for the quenched central galaxies, which is a decrease of ~ 5 times in the relative assembly-type bias on this population when low-mass central galaxies near massive systems are not considered in the clustering estimations.

4.2. Equal samples of quenched and star-forming central galaxies

The results presented in Sect. 4.1 are strongly weighted by the dominant number of central galaxies in the star-forming samples compared to the quenched samples. One may argue that comparing the cross-correlations between both samples is not “fair” due to the differences in number. Studies of assembly bias typically use samples of similar or equal numbers of halos/galaxies in the extremes of the distributions of secondary parameters. To evaluate the consistency of the results of Sect. 4.1 with the literature, we here use the 10 percent of the most quenched central galaxies and the 10 percent of the most star-forming central galaxies in the halo mass range of $10^{11.6}$ and $10^{11.8} h^{-1} M_{\odot}$. This way, we have the same number of central galaxies in both samples, including and excluding galaxies close to massive halos. There are 273,655 quenched central galaxies and the same number of star-forming centrals in the case “PrimAll”, while this number decreases to 169,893 central galaxies for each sample of quenched and star-forming galaxies in the case “PrimB”.

Figure 3 shows the cross-correlations functions of these samples for the cases “PrimAll” and “PrimB”. The autocorrelations of these cases are also shown, which are the same as Fig. 2 by definition, and we use the same symbols and line styles as in that figure. It is now clear the separation in the clustering of both the most quenched and the most star-forming central galaxies with respect to the autocorrelation function of all the central galaxies at fixed halo mass in the case “PrimAll”, i.e., an assembly-type bias, with a higher and lower clustering respectively, as also shown in solid lines in the sub-panel of the figure. This behavior is due to the high star formation sample including fewer SF galaxies than in the previous case, but also with slightly higher sSFRs on average, and the least star forming counterpart containing the quiescent galaxies of Section 4.1. The clustering of the

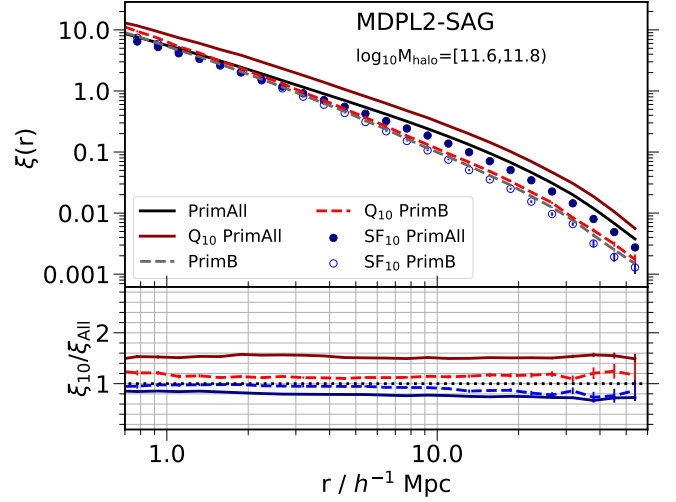


Fig. 3. Same as Fig. 2, but the cross-correlations for the cases “PrimAll” and “PrimB” are between the respective 10% of the most quenched or the 10% of the most star-forming galaxies and the respective full primary sample.

10% most quenched galaxies is, on average, about 50% higher than all the central galaxies between 1 and 50 h^{-1} Mpc, whereas it is about 25% lower for the most star-forming central galaxies.

When central galaxies in the vicinity of galaxy groups and clusters are not used in the estimations, the clustering of the most quenched galaxies is about 15% higher, whereas it is 10% lower for the most star-forming galaxies, on average between 1 and 50 h^{-1} Mpc with respect to all the central galaxies in the case “PrimB”. The above means a decrease of a factor of three in the relative assembly-type bias for equal samples of quenched and star-forming central galaxies. We notice a slight increase in the ratios of “PrimB” galaxies at scales above $\sim 10 h^{-1}$ Mpc. We will come back to this further below.

We confirmed that the distributions for the respective quenched and star-forming samples are similar between the cases “PrimAll” and “PrimB”. The median $\log_{10}(\text{sSFR} / h \text{ yr}^{-1})$ is -10.00 (-9.29) and -9.91 (-9.27) for the 10% of the most Q (SF) centrals in the “PrimAll” and “PrimB” samples, respectively. Therefore, the differences in the clustering between the “PrimAll” and “PrimB” are not due to different sSFR of the chosen quenched and star-forming samples.

The assembly-type bias is strongly reduced in the case “PrimB” when separating the samples according to their sSFR. We observe a similar decrease of the two-halo conformity signal using these samples of primary galaxies (see the dashed lines in the left panel of Fig. A.1). It seems that low-mass central galaxies in the vicinity of groups and clusters, responsible for the two-halo conformity, might be able to explain the assembly-type bias partially, but not all of it. The following section studies the signal strength based on another galaxy property, the stellar age.

4.3. Separating samples of central galaxies according to their stellar ages

We have shown that central galaxies responsible for the two-halo conformity in the low-mass regime can mostly account for the assembly-type bias signal at separations of dozens of Mpc. The signals measured in Figs. 2 and 3 were estimated after separating the sample of central galaxies at fixed halo mass according to

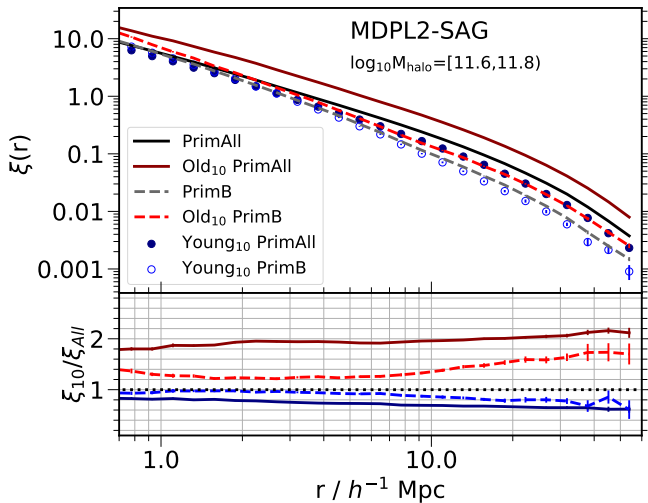


Fig. 4. Similar to Fig. 3, but the cross-correlations for the cases “PrimAll” and “PrimB” are between the respective 10% of the oldest or the 10% of the youngest central galaxies and the respective full primary sample.

their sSFR. However, the sSFR might not be the best tracer of the host halo formation time, a secondary halo property that exhibits strong assembly bias in low-mass DM halos, since it quantifies the level of recent star formation in galaxies.

As suggested by [Lacerna & Padilla \(2011\)](#), a better observational tracer for the halo formation time at fixed halo mass is the stellar age. Therefore, in this section we measure the signal of assembly-type bias for the fiducial case “PrimAll” and the case without central galaxies in the vicinity of massive structures “PrimB” but using the stellar age of the central galaxies. For each case, we separate the 10 percent of the oldest and 10 percent of the youngest galaxies. The correlation functions are shown in Fig. 4. The difference in clustering between the oldest and youngest galaxies in the fiducial case (dark red and navy blue solid lines) is much stronger than between the most quenched and star-forming galaxies (Fig. 3), which confirms that the stellar age is a better proxy for the halo formation time than the sSFR. The clustering of the oldest galaxies is, on average, about 2 times higher than for the case of all the central galaxies between 1 and $50 h^{-1}$ Mpc, whereas it is about 30% lower for the youngest central galaxies. In the case “PrimB” (dashed lines), the clustering between the oldest and youngest galaxies drastically reduces between 1 and $\sim 10 h^{-1}$ Mpc by a factor of ~ 4 . However, the assembly-type bias becomes stronger at larger separations in a clearer way than we found for samples separated according to their sSFR. We will concentrate on a possible explanation for this in the following subsection. We confirmed that the two-halo conformity signal using these samples of primary galaxies also correlates with the assembly-type bias of Fig. 4 (see the right panel of Fig. A.1). The fiducial case “PrimAll” exhibits a stronger conformity signal when separating the central galaxies according to their stellar age than to their sSFR. The conformity signal is notably reduced for the samples “PrimB”, but the residual signal is higher when separating for the stellar age than for the sSFR.

We checked that the change in clustering is not due to a substantial change in the stellar age distributions of the oldest or youngest primary galaxies between the cases “PrimAll” and “PrimB”. The median stellar age of the 10 percent of the old-

est galaxies in “PrimAll” is 3.47 Gyr, whereas it is 3.26 Gyr in “PrimB”. In the case of the 10 percent of the youngest central galaxies, the median age is 1.98 Gyr in “PrimAll”, whereas it is 1.93 Gyr in “PrimB”. The stellar ages are slightly younger when the central galaxies in the vicinity of massive structures are not considered compared with the fiducial case, but not more than 200 Myr on average. This result shows that the different amplitudes of assembly bias between the “PrimAll” and “PrimB” are not due to the difference in stellar age of the chosen old and young subsamples.

4.4. Effect of removal of galaxies around massive halos

We found that the low-mass central galaxies in the vicinity of massive galaxy groups and clusters have, in addition to their contribution to the two-halo galactic conformity, an important role in the assembly-type bias of central galaxies at fixed halo mass at a separation of dozens of megaparsecs. The signal of assembly-type bias decreases by a factor of three to four if they are not included in the clustering estimations (case “PrimB”), with a possible slight increase around $10 h^{-1}$ Mpc. In particular, the results of Fig. 4, when separating between the 10% of the oldest and the 10% of the youngest galaxies, show the most noticeable increase in the signal at these large separations, reaching a clustering similar to the fiducial case (“PrimAll”) at $r > 50 h^{-1}$ Mpc within the error bars.

The case “PrimB” is based on removing central galaxies near massive halos out to clustercentric distances of $5 h^{-1}$ Mpc. It is of interest to check whether there is a particular set of scales in which the clustering of the remaining central galaxies is affected by the massive halos located at the center of the removed regions. To quantify the impact in the selection of this region, we randomly move the position of dark matter halos with masses $M_h \geq 10^{13} h^{-1} M_\odot$ by a fixed distance of $5 h^{-1}$ Mpc from the original positions. We then estimate the cross-correlation function between the “PrimB” sample and the massive halos with the original and the new halo positions. The result is shown in Fig. 5. The clustering with the original and random positions of massive halos (gray dashed and green dot-dashed lines, respectively) differs at separations smaller than $10 h^{-1}$ Mpc, with the clustering of the sample with displaced halos being lower than the original one, until they tend to similar amplitudes at separations larger than $10 h^{-1}$ Mpc. This is the same scale on which we observe an increase in the assembly-type bias strength in the case “PrimB”.

The same clustering at separations larger than $10 h^{-1}$ Mpc, regardless of the exact position of massive halos, means that there is a large-scale correlation with them that is still present in the correlation function even when massive halos are moved to a distance of $5 h^{-1}$ Mpc from their original positions. Therefore, although the short-range effect of assembly-type bias is removed in “PrimB”, there is still an excess of clustering due to the presence of massive halos at larger scales contributing to the signal. The increase of the assembly-type bias signal at large separations is less clearly seen in the case where samples are divided according to their sSFR, but in these cases, error bars are large at large separations.

It is interesting to note that this type of selection could produce a scale-dependent bias. It is possible that some galaxy selections targeting, for instance, samples of emission-lines galaxies, could be affected in a similar way. In particular, emission line galaxies could avoid high-density regions dominated by quenched objects but still be affected by modes produced by massive clusters of galaxies.

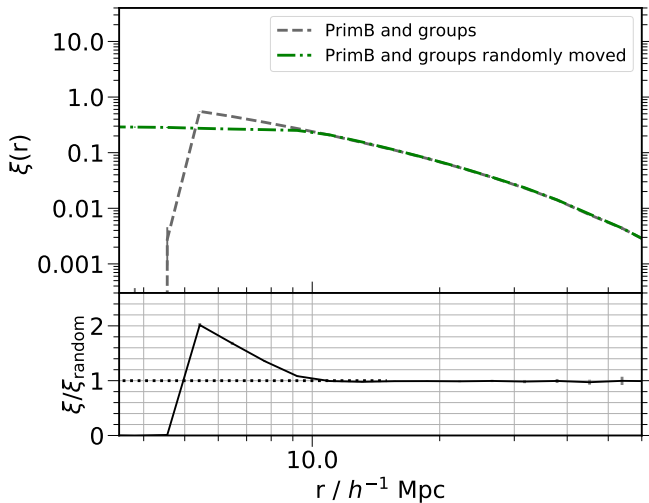


Fig. 5. Cross-correlation function between the “PrimB” sample and the groups and clusters with masses above $10^{13} h^{-1} M_{\odot}$ (gray dashed line). The green dot-dashed line corresponds to the cross-correlation that uses random positions of massive halos with a vector of $5 h^{-1}$ Mpc length from the original positions. The sub-panel shows the ratio between the correlation functions using the original and random positions of massive halos. They are the same at scales larger than $10 h^{-1}$ Mpc.

5. Discussion and conclusions

Environmental effects in the vicinity of massive galaxy groups and clusters seem to cause a significant fraction of two apparently different phenomena: two-halo galactic conformity and assembly-type bias. The former is a term used to describe the correlation between color or star formation activity in low-mass central galaxies and neighboring galaxies in adjacent halos at separations of several megaparsecs, whereas the latter is the secondary halo bias reflected in the large-scale clustering of central galaxies. We evaluated the actual level of equivalence between both phenomena using the MDPL2-SAG galaxy catalog constructed by combining the semi-analytic model of galaxy formation SAG with the dark matter only MultiDark Planck 2 (MDPL2) cosmological simulation.

We focused on synthetic central galaxies at $z = 0$ hosted by low-mass halos of $10^{11.6} \leq M_h/h^{-1} M_{\odot} < 10^{11.8}$ because it is a mass range where the assembly-type bias has been reported to be strong. We referred to the fiducial primary sample with *all* the central galaxies at fixed halo mass as “PrimAll”. We used an additional sample of primary galaxies away from massive halos referred to as “PrimB”, which does not include central galaxies around massive systems of $M_h \geq 10^{13} h^{-1} M_{\odot}$ out to a cluster-centric distance of $5 h^{-1}$ Mpc.

The mean fraction of quenched neighboring galaxies at distances between ~ 1 and $6 h^{-1}$ Mpc from primary galaxies is much higher around quenched centrals than around star-forming centrals in the fiducial case, which implies a strong signal of conformity at fixed halo mass. In contrast, the two-halo conformity signal of the case “PrimB” is always very low at distances $r \gtrsim 1 h^{-1}$ Mpc (Fig. 1). We measured the two-point cross-correlation functions for the fiducial case “PrimAll” and for the case “PrimB”, which excludes low-mass central galaxies in the vicinity of massive structures. The ratio between the correlation function of quenched “PrimAll” galaxies and the total population of central galaxies at fixed halo mass is a factor greater than 2, implying a strong secondary bias on this popu-

lation. We found that the relative assembly-type bias decreases about 5 times on average between 1 and $50 h^{-1}$ Mpc when low-mass central galaxies near massive systems are not considered in the clustering estimations (Fig. 2). Therefore, both the galactic conformity and the assembly-type bias are strongly produced by quenched low-mass central galaxies near massive halos.

The fraction of quenched central galaxies is 1.5% in the halo mass regime studied. When separating the samples of quenched and star-forming galaxies with the same fraction (10% in our case) as is usually done in the literature on the secondary bias, the relative assembly-type bias decreases about 3 times in the case “PrimB” compared to the fiducial case “PrimAll” (Fig. 3). Still, the case “PrimB” shows that the clustering of the most quenched galaxies is about 15% higher, whereas it is 10% lower for the most star-forming galaxies, on average between 1 and $50 h^{-1}$ Mpc with respect to all the central galaxies. Therefore, low-mass central galaxies in the vicinity of groups and clusters, responsible for the two-halo conformity, might be able to explain the assembly-type bias partially, but not all of it. When looking at the conformity signal for these samples, we do find a strong conformity signal for “PrimAll” and, after removing galaxies close to massive halos, the conformity signal decreases less than for the case “PrimB” shown in Fig. 1 between 1 and $1.5 h^{-1}$ Mpc. We show the corresponding conformity signals in the Appendix in the left panel of Fig. A.1. The higher two-halo conformity signal at those scales with the same fractions of Q and SF “PrimB” galaxies compared to the case separating between Q and SF galaxies resembles the higher assembly-type bias for the former samples than the latter.

We also separated the samples according to their stellar age because it has been proposed as a better observational tracer for the halo formation time at fixed halo mass. We confirmed that the stellar age is a better proxy for the halo formation time than the sSFR because the difference in clustering between the oldest and youngest galaxies in the fiducial case (“PrimAll”, Fig. 4) is much stronger than between the most quenched and star-forming central galaxies. The clustering between the oldest and youngest galaxies drastically reduces by a factor of ~ 4 between 1 and $\sim 10 h^{-1}$ Mpc in the case “PrimB”. However, the assembly-type bias becomes stronger at larger separations, reaching a clustering similar to the fiducial case at $r > 50 h^{-1}$ Mpc. We quantified the impact of removing low-mass central galaxies near groups and clusters by randomly moving the position of massive halos by a fixed distance of $5 h^{-1}$ Mpc from their original positions. The cross-correlation function between the “PrimB” sample and the massive halos with their original and random positions becomes equal at separations larger than $10 h^{-1}$ Mpc (Fig. 5), which is the same scale with the increase in the assembly-type bias strength seen in the case “PrimB”. Therefore, there is an excess of clustering due to the presence of massive halos at scales larger than $10 h^{-1}$ Mpc contributing to the signal. Again, we repeat the measurement of the quenched fraction of neighboring galaxies as a function of distance for this set of primary samples and show the results in the Appendix, in the right panel of Fig. A.1. As can be seen, the signal of conformity around “PrimAll” and “PrimB” central galaxies with old and young stellar populations is higher than for the selection of samples using sSFR, mirroring the relative amplitudes of assembly-type bias for these two sets of samples.

The low mass assembly-type bias that we measured can be explained by three causes, according to Mansfield & Kravtsov (2020): large-scale tidal fields, gravitational heating due to the collapse of large-scale structures, and splashback subhaloes located outside the virial radius. Palma et al. (2025) showed that

the splashback galaxies do not affect the conformity signal in the MDPL2-SAG model. Therefore, it is likely that the correlation between conformity and low-mass assembly-type bias is mainly given by tidal forces and gravitational heating occurring in similar large-scale structures such as filaments. These two effects can truncate the mass accretion histories of low-mass halos (e.g., [Mansfield & Kravtsov 2020](#)).

Notably, the assembly-type bias is strongest for the fiducial samples, also showing the strongest conformity signal. This result suggests that there could exist a direct relation between the amplitude of these two effects. If two-halo conformity is confirmed with observational samples as shown, for example, by [Ayromlou et al. \(2023\)](#) using SDSS ([Abazajian et al. 2009](#)) and dark energy spectroscopic instrument (DESI, [Dey et al. 2019](#); [Zou et al. 2019](#)) samples, it could be taken as an indication of assembly-type bias in the real Universe.

Acknowledgements. We would like to thank Antonio Montero-Dorta, Sergio Contreras, Vladimir Avila-Reese, Raúl Angulo, Aldo Rodríguez-Puebla, Simon White, Doris Stoppacher, and Nely Choque-Challapa for comments and discussions. We also thank Andrés Ruiz, Yamila Yaryura and Cristian Vega for their support in organizing and providing the MDPL2-SAG data used in this work. NP acknowledges support from Agencia Nacional de Investigación Científica y Tecnológica through grants PICT-2021-0700 and PICT-2023-0002. DP acknowledges the support through ANID-Subdirección de Capital Humano/Doctorado Nacional/2024/21241817.

References

- Abazajian, K. N., Adelman-McCarthy, J. K., Agüeros, M. A., et al. 2009, *ApJS*, 182, 543
- Alam, S., Peacock, J. A., Kraljic, K., Ross, A. J., & Comparat, J. 2020, *MNRAS*, 497, 581
- Argudo-Fernández, M., Lacerna, I., & Duarte Puertas, S. 2018, *A&A*, 620, A113
- Artale, M. C., Zehavi, I., Contreras, S., & Norberg, P. 2018, *MNRAS*, 480, 3978
- Ayromlou, M., Kauffmann, G., Anand, A., & White, S. D. M. 2023, *MNRAS*, 519, 1913
- Ayromlou, M., Kauffmann, G., Yates, R. M., Nelson, D., & White, S. D. M. 2021, *MNRAS*, 505, 492
- Bahé, Y. M., Barnes, D. J., Dalla Vecchia, C., et al. 2017, *MNRAS*, 470, 4186
- Bahé, Y. M., McCarthy, I. G., Balogh, M. L., & Font, A. S. 2013, *MNRAS*, 430, 3017
- Behroozi, P. S., Wechsler, R. H., & Wu, H.-Y. 2013, *ApJ*, 762, 109
- Benítez-Llambay, A., Navarro, J. F., Abadi, M. G., et al. 2013, *ApJ*, 763, L41
- Berti, A. M., Coil, A. L., Behroozi, P. S., et al. 2017, *ApJ*, 834, 87
- Blanton, M. R., Schlegel, D. J., Strauss, M. A., et al. 2005, *AJ*, 129, 2562
- Bluck, A. F. L., Mendel, J. T., Ellison, S. L., et al. 2014, *MNRAS*, 441, 599
- Bray, A. D., Pillepich, A., Sales, L. V., et al. 2016, *MNRAS*, 455, 185
- Brown, T., Catinella, B., Cortese, L., et al. 2017, *MNRAS*, 466, 1275
- Calderon, V. F., Berlind, A. A., & Sinha, M. 2018, *MNRAS*, 480, 2031
- Campbell, D., van den Bosch, F. C., Hearin, A., et al. 2015, *MNRAS*, 452, 444
- Contreras, S., Zehavi, I., Padilla, N., et al. 2019, *MNRAS*, 484, 1133
- Cooper, M. C., Gallazzi, A., Newman, J. A., & Yan, R. 2010, *MNRAS*, 402, 1942
- Cora, S. A., Vega-Martínez, C. A., Hough, T., et al. 2018, *MNRAS*, 479, 2
- Croton, D. J., Gao, L., & White, S. D. M. 2007, *MNRAS*, 374, 1303
- Cybulski, R., Yun, M. S., Fazio, G. G., & Gutermuth, R. A. 2014, *MNRAS*, 439, 3564
- Dalal, N., White, M., Bond, J. R., & Shirokov, A. 2008, *ApJ*, 687, 12
- Damsted, S., Finoguenov, A., Lietzen, H., et al. 2024, *A&A*, 690, A52
- Dey, A., Schlegel, D. J., Lang, D., et al. 2019, *AJ*, 157, 168
- Duckworth, C., Tojeiro, R., Kraljic, K., et al. 2019, *MNRAS*, 483, 172
- Dvornik, A., Cacciato, M., Kuijken, K., et al. 2017, *MNRAS*, 468, 3251
- Gao, L., Springel, V., & White, S. D. M. 2005, *MNRAS*, 363, L66
- García-Quintero, C., Mena-Fernández, J., Rocher, A., et al. 2025, *J. Cosmology Astropart. Phys.*, 2025, 132
- Goddard, D., Thomas, D., Maraston, C., et al. 2017, *MNRAS*, 465, 688
- Hadzhiyska, B., Eisenstein, D., Hernquist, L., et al. 2023, *MNRAS*, 524, 2507
- Hahn, O., Porciani, C., Dekel, A., & Carollo, C. M. 2009, *MNRAS*, 398, 1742
- Hearin, A. P., Behroozi, P. S., & van den Bosch, F. C. 2016, *MNRAS*, 461, 2135
- Hearin, A. P., Watson, D. F., & van den Bosch, F. C. 2015, *MNRAS*, 452, 1958
- Hough, T., Cora, S. A., Haggard, R., et al. 2023, *MNRAS*, 518, 2398
- Kauffmann, G. 2015, *MNRAS*, 454, 1840
- Kauffmann, G., Li, C., Zhang, W., & Weinmann, S. 2013, *MNRAS*, 430, 1447
- Klypin, A., Yepes, G., Gottlöber, S., Prada, F., & Heß, S. 2016, *MNRAS*, 457, 4340
- Knebe, A., Stoppacher, D., Prada, F., et al. 2018, *MNRAS*, 474, 5206
- Kraljic, K., Pichon, C., Dubois, Y., et al. 2019, *MNRAS*, 483, 3227
- Kuutma, T., Tamm, A., & Tempel, E. 2017, *A&A*, 600, L6
- Lacerna, I., Contreras, S., González, R. E., Padilla, N., & Gonzalez-Perez, V. 2018, *MNRAS*, 475, 1177
- Lacerna, I. & Padilla, N. 2011, *MNRAS*, 412, 1283
- Lacerna, I., Padilla, N., & Stasyszyn, F. 2014, *MNRAS*, 443, 3107
- Lacerna, I., Rodriguez, F., Montero-Dorta, A. D., et al. 2022, *MNRAS*, 513, 2271
- Landy, S. D. & Szalay, A. S. 1993, *ApJ*, 412, 64
- Li, L.-C., Qin, B., Wang, J., Wang, J., & Wang, Y.-G. 2021, *Research in Astronomy and Astrophysics*, 21, 032
- Li, Y., Mo, H. J., & Gao, L. 2008, *MNRAS*, 389, 1419
- Lin, Y.-T., Mandelbaum, R., Huang, Y.-H., et al. 2016, *ApJ*, 819, 119
- Lin, Y.-T., Miyatake, H., Guo, H., et al. 2022, *A&A*, 666, A97
- Mansfield, P. & Kravtsov, A. V. 2020, *MNRAS*, 493, 4763
- Marinacci, F., Vogelsberger, M., Pakmor, R., et al. 2018, *MNRAS*, 480, 5113
- McConachie, I., Wilson, G., Forrest, B., et al. 2025, *ApJ*, 978, 17
- Montero-Dorta, A. D., Artale, M. C., Abramo, L. R., et al. 2020, *MNRAS*, 496, 1182
- Naiman, J. P., Pillepich, A., Springel, V., et al. 2018, *MNRAS*, 477, 1206
- Nelson, D., Pillepich, A., Springel, V., et al. 2018, *MNRAS*, 475, 624
- Nelson, D., Springel, V., Pillepich, A., et al. 2019, *Computational Astrophysics and Cosmology*, 6, 2
- Norberg, P., Baugh, C. M., Gaztañaga, E., & Croton, D. J. 2009, *MNRAS*, 396, 19
- Olsen, C. & Gawiser, E. 2023, *ApJ*, 943, 30
- Ortega-Martínez, S., Contreras, S., Angulo, R. E., & Chaves-Montero, J. 2024, *arXiv e-prints*, arXiv:2411.11830
- Oyarzún, G. A., Bundy, K., Westfall, K. B., et al. 2022, *ApJ*, 933, 88
- Oyarzún, G. A., Tinker, J. L., Bundy, K., Xhakaj, E., & Wyithe, J. S. B. 2024, *ApJ*, 974, 29
- Pallero, D., Gómez, F. A., Padilla, N. D., et al. 2019, *MNRAS*, 488, 847
- Palma, D., Lacerna, I., Celeste Artale, M., et al. 2025, *A&A*, 693, A67
- Pandey, B. & Sarkar, S. 2020, *MNRAS*, 498, 6069
- Paranjape, A., Kovač, K., Hartley, W. G., & Pahwa, I. 2015, *MNRAS*, 454, 3030
- Peng, Y.-j., Lilly, S. J., Kovač, K., et al. 2010, *ApJ*, 721, 193
- Pillepich, A., Springel, V., Nelson, D., et al. 2018, *MNRAS*, 473, 4077
- Planck Collaboration, Ade, P. A. R., Aghanim, N., et al. 2014, *A&A*, 571, A16
- Rafieeantsoa, M. & Davé, R. 2018, *MNRAS*, 475, 955
- Salcedo, A. N., Maller, A. H., Berlind, A. A., et al. 2018, *MNRAS*, 475, 4411
- Sin, L. P. T., Lilly, S. J., & Henriques, B. M. B. 2017, *MNRAS*, 471, 1192
- Sin, L. P. T., Lilly, S. J., & Henriques, B. M. B. 2019, *MNRAS*, 488, 234
- Sinha, M. & Garrison, L. 2017, *Corfunc: Blazing fast correlation functions on the CPU*, *Astrophysics Source Code Library*, record ascl:1703.003
- Sinha, M. & Garrison, L. 2019, in *Software Challenges to Exascale Computing*, ed. A. Majumdar & R. Arora (Singapore: Springer Singapore), 3–20
- Sinha, M. & Garrison, L. H. 2020, *MNRAS*, 491, 3022
- Skibba, R., Sheth, R. K., Connolly, A. J., & Scranton, R. 2006, *MNRAS*, 369, 68
- Smith, W. J., Berlind, A. A., & Sinha, M. 2024, *MNRAS*, 535, 1426
- Springel, V., Pakmor, R., Pillepich, A., et al. 2018, *MNRAS*, 475, 676
- Sun, S., Guo, Q., Wang, L., et al. 2018, *MNRAS*, 477, 3136
- Tinker, J. L., Hahn, C., Mao, Y.-Y., Wetzel, A. R., & Conroy, C. 2018, *MNRAS*, 477, 935
- Tremmel, M., Quinn, T. R., Ricarte, A., et al. 2019, *MNRAS*, 483, 3336
- Treyer, M., Kraljic, K., Arnouts, S., et al. 2018, *MNRAS*, 477, 2684
- Wang, K., Peng, Y., & Chen, Y. 2023, *MNRAS*, 523, 1268
- Wang, L., De Lucia, G., & Weinmann, S. M. 2013a, *MNRAS*, 431, 600
- Wang, L., Weinmann, S. M., De Lucia, G., & Yang, X. 2013b, *MNRAS*, 433, 515
- Wechsler, R. H. & Tinker, J. L. 2018, *ARA&A*, 56, 435
- Wetzel, A. R., Tinker, J. L., & Conroy, C. 2012, *MNRAS*, 424, 232
- York, D. G., Adelman, J., Anderson, Jr., J. E., Anderson, S. F., & et al. 2000, *AJ*, 120, 1579
- Zehavi, I., Blanton, M. R., Frieman, J. A., et al. 2002, *ApJ*, 571, 172
- Zehavi, I., Contreras, S., Padilla, N., et al. 2018, *ApJ*, 853, 84
- Zhang, Y., Yang, X., & Guo, H. 2021, *MNRAS*, 507, 5320
- Zheng, Z., Li, C., Mao, S., et al. 2019, *ApJ*, 873, 63
- Zheng, Z., Wang, H., Ge, J., et al. 2017, *MNRAS*, 465, 4572
- Zinger, E., Dekel, A., Kravtsov, A. V., & Nagai, D. 2018, *MNRAS*, 475, 3654
- Zou, H., Gao, J., Zhou, X., & Kong, X. 2019, *ApJS*, 242, 8
- Zu, Y. & Mandelbaum, R. 2018, *MNRAS*, 476, 1637

Appendix A: Two-halo conformity separating primary samples in ranges of sSFR and stellar age

We showed in Sect. 3 that the signal of two-halo galactic conformity when the primary samples are separated between quenched and star-forming central galaxies. Fig. A.1 shows the results when the primary samples are separated using the conditions of Sects. 4.2 and 4.3, that is, with the 10 percent of the most quenched and the 10 percent of the most star-forming central galaxies and using the 10 percent of the oldest and the 10 percent of the youngest galaxies in the same host halo mass range, respectively. In this way, we can assess whether the conformity signal varies as the assembly-type bias signal does using these conditions. We maintain the secondary galaxies are quenched if $\text{sSFR} \leq 10^{-10.5} h \text{ yr}^{-1}$.

The left panel corresponds to the separation between the most quenched and the most star-forming central galaxies. The quenched fractions of neighboring (secondary) galaxies decrease around primary galaxies in the case “PrimAll” (dark red and navy blue solid lines) compared to the results in Fig. 1. The conformity signal (black solid line) also decreases from $\Delta f_Q = 0.22$ to 0.15 at separations of $r \sim 1 h^{-1} \text{ Mpc}$, but it is relatively strong out to distances $r \lesssim 4 h^{-1} \text{ Mpc}$ with $\Delta f_Q > 0.04$. This lower signal is expected because 10 percent of the most quenched primary galaxies include centrals with $\text{sSFR} > 10^{-10.5} h \text{ yr}^{-1}$. On the other hand, the conformity signal for the case “PrimB” is similar to that shown in Fig. 1, although with slightly higher values of $\Delta f_Q \sim 0.03$ at separations between 1 and $1.5 h^{-1} \text{ Mpc}$.

The right panel of Fig. A.1 corresponds to the separation between the oldest and the youngest central galaxies. The quenched fractions of neighboring galaxies also decrease around primary galaxies in the case “PrimAll” compared to the results in Fig. 1. The conformity signal (black solid line) decreases from $\Delta f_Q = 0.22$ to 0.18 at separations of $r \sim 1 h^{-1} \text{ Mpc}$. It is relatively strong out to distances $r \lesssim 7 h^{-1} \text{ Mpc}$ with $\Delta f_Q \gtrsim 0.04$. Therefore, the conformity signal is stronger after separating the (fiducial) primary sample in stellar age than in sSFR. This result is consistent with that of Sect. 4, in which the assembly-type bias is stronger using the stellar age compared to the sSFR.

In contrast to the left panel of A.1, the right panel shows an evident two-halo conformity signal for the case “PrimB” at separations $r \lesssim 2 h^{-1} \text{ Mpc}$. This result is mainly produced by the higher neighbor quenched fraction around the oldest primary galaxies (red dashed line). We notice that 10 percent of the oldest “PrimB” galaxies have a median stellar age of 3.3 Gyr, which also include many star-forming galaxies with $\text{sSFR} > 10^{-10.5} h \text{ yr}^{-1}$, which are not part of the 10 percent of the most quenched galaxies. Nonetheless, the conformity signal decreases notably in the case “PrimB” compared to the fiducial case “PrimAll” at $r \geq 1 h^{-1} \text{ Mpc}$.

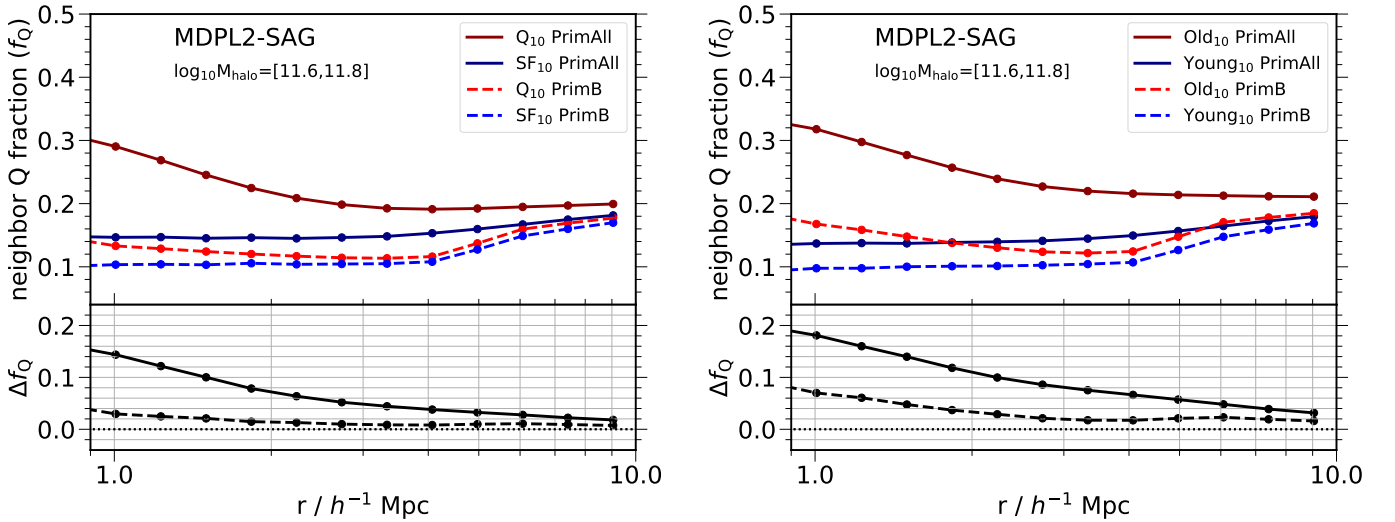


Fig. A.1. Same as Fig. 1, but the primary samples are separated between the 10 percent of the most quenched and the 10 percent of the most star-forming central galaxies (left) and between the 10 percent of the oldest and 10 percent of the youngest central galaxies (right).